Candidalysin: A fungal peptide toxin critical for mucosal infection

David L. Moyes[1*], Duncan Wilson[2*ǂ], Jonathan P. Richardson[1*], Selene Mogavero[2*], Shirley X. Tang[1], Julia Wernecke[3,4], Sarah Höfs[2], Remi L. Gratacap[5], Jon Robbins[6], Manohursingh Runglall[1ǂǂ], Celia Murciano[1ǂǂ], Mariana Blagojevic[1], Selvam Thavaraj[1], Toni M. Förster[2], Betty Hebecker[2,7], Lydia Kasper[2], Gema Vizcay[8], Simona I. Iancu[1], Nessim Kichik[1,9], Antje Häder[10], Oliver Kurzai[10], Ting Luo[11], Thomas Krueger[11], Olaf Kniemeyer[11], Ernesto Cota[9], Oliver Bader[12], Robert T. Wheeler[5], Thomas Gutsmann[3], Bernhard Hube[2,13,14] and Julian R. Naglik[1]

[1] Mucosal & Salivary Biology Division, Dental Institute, King's College London, UK
[2] Department of Microbial Pathogenicity Mechanisms, Hans Knoell Institute, Jena, Germany
[3] Research Center Borstel, Division of Biophysics, Borstel, Germany
[4] Deutsches Elektronen-Synchrotron DESY, Hamburg, Germany
[5] Department of Molecular & Biomedical Sciences, University of Maine, Orono, ME, USA
[6] Wolfson CARD, King's College, Guy's Campus, London, UK
[7] Research Group Microbial Immunology, Hans Knoell Institute, Jena, Germany
[8] Centre for Ultrastructural Imaging, King's College London, UK
[9] Department of Life Sciences, Imperial College London, London, UK
[10] Septomics Research Center, Hans-Knoell Institute and Friedrich Schiller University, Jena
[11] Department of Molecular and Applied Microbiology, Hans Knoell Institute, Jena, Germany
[12] Institute for Medical Microbiology, University Medical Center Göttingen, Göttingen, Germany
[13] Friedrich Schiller University, Jena, Germany
[14] Integrated Research and Treatment Center, Center for Sepsis Control and Care, Jena, Germany
* These authors contributed equally to this work.

Current address:
ǂ Aberdeen Fungal Group, School of Medical Sciences, University of Aberdeen, Aberdeen, UK
ǂǂ NIHR Biomedical Research Centre, Guy's and St Thomas' NHS Foundation Trust, London, UK

34 ## ERI Biotecmed & Microbiology and Ecology Department, University of Valencia, Valencia,
35 Spain

Abstract

Cytolytic proteins and peptide toxins are classical virulence factors of several bacterial pathogens which disrupt epithelial barrier function, damage cells and activate or modulate host immune responses[1,2]. Here we identify the first cytolytic peptide toxin in a human pathogenic fungus. This peptide (Ece1-III) is generated from a parent protein, Ece1p, and is produced by the invasive hyphal form of the opportunistic fungal pathogen *Candida albicans*. Ece1-III directly damages epithelial membranes and, at sub-lytic concentrations, triggers a danger response pathway, activating epithelial immunity. *C. albicans* strains lacking Ece1-III do not activate or damage epithelial cells and are avirulent in animal models of mucosal infection. This amphipathic peptide adopts an α-helical structure that causes cytolysis of multiple human epithelial cell types. Membrane permeabilization is enhanced by a positively charged C-terminus and triggers an inward current concomitant with calcium influx. Given its cytolytic activity, we propose the name 'Candidalysin' for Ece1-III. Candidalysin is the first described cytolytic peptide toxin of a human fungal pathogen and is a critical molecular determinant of epithelial damage and host recognition of the clinically important fungus, *C. albicans*.

Results

Normally a benign member of human microbiota, *Candida albicans* is responsible for millions of mucosal infections each year, often with severe morbidity[3]. A defining feature of *C. albicans* pathogenesis is the transition from yeast to invasive filamentous hyphae. Hyphae damage mucosal epithelia and induce activation of the the activating protein-1 (AP-1) transcription factor c-Fos (via p38-MAPK) and the MAPK phosphatase MKP1 (via ERK1/2-MAPK), which trigger pro-inflammatory cytokine responses[4,5]. These signaling events constitute a 'danger response' against invasive hyphae, thus serving as a sensor of pathogenic *C. albicans* invasion [6,7].

Despite the well-known association between filamentation and virulence, the molecular mechanism underlying hypha-driven epithelial activation and mucosal damage has remained obscure. To elucidate this mechanism, we screened a panel of *C. albicans* gene deletion mutants that targeted key processes, pathways and proteins known or predicted to be associated with the yeast-hyphal transition and pathogenicity (n = 62). Only hypha-producing strains induced MKP1 phosphorylation (p-MKP1), c-Fos, cytokines (IL-1α, IL-6, G-CSF) and damage in oral epithelial cells (Extended Data Table 1). However, one *C.albicans* mutant (*ece1*Δ/Δ)[8] formed normal hyphae but was incapable of inducing these epithelial danger responses. *C.*

albicans ECE1 (extent of cell elongation) is highly expressed by hyphae during epithelial infection (Extended Data Fig. 1a, b) and is predicted to encode a secreted protein[9]. To probe its function we generated a panel of *C. albicans ECE1*-mutants (Extended Data Table 2). The *ece1*Δ/Δ strain formed normal hyphae (Extended Data Fig. 1c), and adhered to and invaded human epithelial cells similarly to wild type *C. albicans* (Extended Data Fig. 1d, e). Indeed, *ece1*Δ/Δ was capable of extensive epithelial invasion, penetrating through epithelial cells (Extended Data Fig. 1f). Despite this, invasive *ece1*Δ/Δ hyphae did not damage epithelia or induce p-MKP1/c-Fos mediated danger responses or cytokine secretion (Fig. 1a-d). Thus, Ece1p is critical for epithelial damage and innate recognition of *C. albicans* hyphae *in vitro*.

We next assessed the role of *ECE1* in two *in vivo* models of *C. albicans* mucosal infection. In murine oropharyngeal candidiasis (OPC)[10], mice infected with *C. albicans* wild type or *ECE1* re-integrant (*ece1*Δ/Δ+*ECE1*) strains exhibited disease symptoms, including extensive hyphal invasion of the tongue epithelium, micro-abscesses of infiltrating neutrophils and tissue damage (Fig. 1e, f, h, i). In contrast, tongue tissue from *ece1*Δ/Δ-infected animals (n = 17/20) showed no invasive fungi and no inflammatory infiltrates or damage (Fig. 1g). We detected very low numbers of *ece1*Δ/Δ in only 3/20 mice (Extended Data Fig. 2a), which showed no evidence of local epithelial damage (not shown). Quantification of histology sections indicated that the percentage of epithelial surface infected was significantly greater with the wild type and *ECE1* re-integrant strains (Extended Data Fig. 2b). In a zebrafish swimbladder model of mucosal infection[11,12], neutrophil recruitment and tissue damage were both significantly lower following *ece1*Δ/Δ infection as compared with the wild type strain (Fig. 1j, k, Extended Data Fig. 2c, d). Therefore, *C. albicans* Ece1p is critical for mucosal pathogenesis and is an innate immune activator *in vivo*.

Ece1p is an *in vitro* substrate for Kex2p, a Golgi-located protease that cleaves proteins after lysine-arginine (KR) motifs[13]. Ece1p contains seven KR-processing sites, indicating that eight peptides are produced and secreted from *C. albicans*[13] (Extended Data Fig. 3a, b). Liquid chromatography–mass spectrometry (LC-MS/MS) analysis confirmed that rKex2p processes rEce1p and all eight peptides terminating in KR (and fragments thereof, showing that less efficient processing occurs also after a single K or R) are generated (Supplementary information). To determine which Ece1p peptide(s) were responsible for epithelial activation and damage, oral epithelial cells were incubated with peptides Ece1-I-VIII (1.5 – 70 μM). Only Ece1-III$_{62\text{-}93}$ induced p-MKP1, c-Fos, cytokines and damage (Fig. 2a-c, Extended Data Fig. 3c-e). Notably, low Ece1-III$_{62\text{-}93}$ concentrations (1.5 – 15 μM) were sufficient to induce c-Fos DNA binding (Fig. 2d), G-CSF and GM-CSF (Fig. 2b, Extended Data Fig. 3c), while high

Ece1-III$_{62-93}$ concentrations (70 μM) were required to induce damage (Fig. 2e) and the damage-associated cytokines IL-1α and IL-6, respectively (Extended Data Fig. 3d, e). Ece1-III$_{62-93}$ could also directly lyse multiple human epithelial cell types and induce hemolysis of red blood cells, a classical test for cytotoxin activity (not shown). Neither the N-terminal hydrophobic region (Ece1-III$_{62-85}$) nor the C-terminal hydrophilic region (Ece1-III$_{86-93}$) induced p-MKP1, c-Fos, cytokines or damage of epithelial cells, either individually or in combination (Extended Data Fig. 3f-h), demonstrating that the peptide containing both regions is required for activity. Therefore, Ece1-III$_{62-93}$ is the active region of Ece1p, acting as an epithelial immune activator and a cytolytic agent.

To confirm that Ece1-III$_{62-93}$ drives epithelial activation and fungal pathogenicity, we generated a *C. albicans* strain lacking only the Ece1-III$_{62-93}$ region (*ece1*Δ/Δ+*ECE1*$_{\Delta 184-279}$). This strain expressed the mutated *ECE1* gene and, like *ece1*Δ/Δ, efficiently formed invasive hyphae (not shown). However, *ece1*Δ/Δ+*ECE1*$_{\Delta 184-279}$ was unable to induce p-MKP1, c-Fos DNA binding, cytokines, or damage epithelia (Fig. 2f-i). In murine OPC, unlike the *ece1*Δ/Δ+*ECE1* recomplemented strain, *ece1*Δ/Δ+*ECE1*$_{\Delta 184-279}$-infected mice demonstrated absent (n = 4/10) or low (n = 6/10) fungal burdens, with no evidence of inflammatory infiltrates or local epithelial damage (Fig. 2j-l, Extended Data Fig. 4a and 4b) Likewise, *ece1*Δ/Δ+*ECE1*$_{\Delta 184-279}$ did not induce full damage in the zebrafish swimbladder model (Fig. 2m, Extended Data Fig. 4c). In contrast, injection of lytic doses of Ece1-III$_{62-93}$ into the swimbladder induced epithelial damage (Fig. 2n, o). Thus, Ece1-III$_{62-93}$ is both necessary and sufficient for epithelial immune activation, damage and mucosal infection *in vivo*. The amphipathic properties of Ece1-III$_{62-93}$ (SIIGIIMGILGNIPQVIQIIMSIVKAFKGNKR) coupled with the α-helical structure of the N-terminal hydrophobic region (Extended Data Fig. 5a, b) indicated that this fungal peptide may act similarly to cationic antimicrobial peptides and peptide toxins such as melittin[14] (honey bee), magainin 2[15] (African clawed frog) and alamethicin[16] (*Trichoderma viride*). Cytolytic peptide toxins have not previously been found in human pathogenic fungi but bacterial cytolytic toxins are known to induce lesions after binding to target cell membranes[1]. To investigate the importance of lipid composition for Ece1-III$_{62-93}$-mediated cytolysis, we used Förster resonance energy transfer (FRET) and electrical impedance spectroscopy to analyze the interactions of Ece1-III$_{62-93}$ with model membranes comprised of lipid bilayers of dioleoylphosphatidylcholine (DOPC) with or without cholesterol. While Ece1-III$_{62-93}$ was able to efficiently intercalate into and permeabilize DOPC membranes, Ece1-III$_{62-93}$ permeabilization was enhanced in the presence of cholesterol (Fig. 3a, Extended Data Fig. 5c). Ece1-III$_{62-93}$-induced lesions were

heterogeneous and transient (Extended Data Fig. 5d), indicating that the peptide may damage target membranes through a 'carpet-like' mechanism[17]. Patch-clamp analysis of epithelial cells demonstrated that lesion formation by Ece1-III$_{62\text{-}93}$ is rapid and causes an inward current (Fig. 3b), associated with calcium influx (Fig. 3c). Similar phenomena occur with bacterial cytolytic toxins, which are known to trigger cell activation[1,2,18].

We postulated that the positively-charged C-terminal KR residues of Ece1-III$_{62\text{-}93}$ might be critical for interacting with negatively-charged components of host membranes to promote lesion formation. Substitution of the KR motif to AA (alanine-alanine; Ece1-III$_{62\text{-}93AA}$) did not affect membrane intercalation (not shown) but significantly reduced the peptide's ability to permeabilize membranes, damage epithelial cells and induce calcium influx (Fig. 3c-e). Thus, the positive C-terminus of Ece1-III$_{62\text{-}93}$ is critical for lesion formation and damage induction in epithelial membranes. Notably, Ece1-III$_{62\text{-}93AA}$ still induced p-MKP1, c-Fos and the non-damage associated cytokine G-CSF (Fig. 3f, g) but not the damage-associated cytokine IL-1α (Fig. 3h), suggesting that Ece1-III$_{62\text{-}93AA}$ can be recognized by epithelial immunity without without damaging cells. This concept is important as it means that epithelial cells are not only responding to damage but have evolved to specifically recognise the peptide.

To demonstrate that Ece1-III is generated during epithelial infection, we performed LC-MS/MS analysis on the secretome from wild-type *C. albicans* hyphae grown in the presence and absence of epithelial cells (Supplementary information). Ece1-III was the only peptide detected in the presence of epithelial cells, indicating that the fungus secretes this toxin during mucosal infection at high concentrations. However, most significantly, the predominant form of secreted Ece1-III terminated in a K residue (SIIGIIMGILGNIPQVIQIIMSIVKAFKGNK; Ece1-III$_{62\text{-}92K}$) and not KR (SIIGIIMGILGNIPQVIQIIMSIVKAFKGNKR; Ece1-III$_{62\text{-}93KR}$) (Extended Data Table 4). In fungi, it is known that following Kex2p processing, many proteins are subsequently cleaved by Kex1p (also in the Golgi), removing the C-terminal R. LC-MS/MS analysis on the hyphal secretome of a *kex1*Δ/Δ mutant demonstrated that here the predominant peptide secreted terminates in KR (not K). Therefore, Ece1 is also subject to ordered Kex2p/Kex1p processing. Accordingly, we confirmed that Ece1-III$_{62\text{-}92K}$ functioned similarly to Ece1-III$_{62\text{-}93KR}$ with respect to epithelial cell activation. Specifically, Ece1-III$_{62\text{-}92K}$ is also α-helical (not shown) and induces c-Fos, p-MKP1, cytokines (IL-1α, G-CSF), damage (LDH), membrane intercalation and permeabilization, and calcium influx (Fig 4a-g). Thus, the dominant peptide secreted from *C. albicans* hyphae during mucosal infection is Ece1-III$_{62\text{-}92K}$, which acts as a cytolytic peptide toxin that activates epithelial cells.

Based on these data, we propose a model of *C. albicans* mucosal infection whereby invasive hyphae secrete Ece1-III$_{62\text{-}92K}$ into a membrane-bound 'invasion pocket'[19], facilitating peptide accumulation (Extended Data Fig 6). During early stages of infection, sub-lytic concentrations of Ece1-III$_{62\text{-}92K}$ induce epithelial immunity by activating the 'danger response' pathway (p-MKP1/c-Fos), alerting the host to the transition from colonizing yeast to invasive, toxin-producing hyphae. As infection progresses, Ece1-III$_{62\text{-}92K}$ levels accumulate and elicit direct tissue damage. Mechanistically, we propose that the asymmetric distribution of charge along the α-helix of Ece1-III$_{62\text{-}92K}$ facilitates correct peptide orientation relative to the host membrane, enabling intercalation, permeabilization and calcium influx. In conclusion, our data identifies *C. albicans* Ece1-III$_{62\text{-}92K}$ as the first cytolytic peptide toxin in a human fungal pathogen and reveals the molecular mechanisms of epithelial damage and host recognition of this clinically important fungus. We propose the name 'Candidalysin' for this newly discovered fungal toxin.

Supplementary Information is available in the online version of the paper.

Acknowledgements We thank Sarah Gaffen, Bruce Klein, Christian Hertweck, Abigail Tucker, Jeremy Green and Stephen Challacombe for comments on the manuscript. For experimental assistance we thank Stuart Bevan and David Andersson (calcium assays), Deepa Nayar (histology), Durdana Rahman and Mukesh Mistry (murine model), Mark Nilan (zebrafish model), Sabrina Groth (FRET spectroscopy), Nadine Gebauer (Impedance experiments), Daniela Schulz (*kex1*Δ/Δ strain) and our colleagues for supplying fungal mutant strains. This work was supported by grants from the Medical Research Council (MR/J008303/1, MR/M011372/1), Biotechnology & Biological Sciences Research Council (BB/J015261/1), FP7-PEOPLE-2013-Initial Training Network (606786) to JRN; Wellcome Trust Strategic Award for Medical Mycology and Fungal Immunology (097377/Z/11/Z) to JRN and DW; Sir Henry Dale Fellowship jointly funded by the Wellcome Trust and the Royal Society (102549/Z/13/Z) to DW; Deutsche Forschungsgemeinschaft CRC/TR124 FungiNet Project C1 and Z2, Deutsche Forschungsgemeinschaft SPP 1580 (Hu 528/17-1) and CSCC, German Federal Ministry of Education and Health [BMBF] 01EO1002 to BH; Cluster of Excellence 'Inflammation at interfaces' and Deutsche Forschungsgemeinschaft SPP1580 project GU 568/5-1 to TG; National Institutes of Health (R15AI094406) and the Burroughs Wellcome Fund to RTW.

Author Contributions DLM, JPR, SXT, MR, CM, MB, SII, NK performed signalling, transcription factor, calcium and cytokine assays, and murine work; DW, SH, SM, TMF, BH, LK AH, OB and OKu created fungal strains and performed fluorescent microscopy, adhesion, invasion, gene expression and damage assays; RLG and RTW performed zebrafish experiments; JW and TG performed biophysical analysis with artificial membranes; JR performed whole patch clamp analysis; GV performed electron microscopy; ST performed histological analysis; SM, TL, TK and OKn performed LC-MS analyses; DLM, JPR, DW, BH and JRN wrote the paper; EC, BH and JRN supervised the project.

Author Information Reprints and permissions information is available at www.nature.com/reprints. The authors declare no competing financial interests. Readers are welcome to comment on the online version of the paper. Correspondence and requests for materials should be addressed to B.H (bernhard.hube@leibniz-hki.de).

References

1 Los, F. C., Randis, T. M., Aroian, R. V. & Ratner, A. J. Role of pore-forming toxins in bacterial infectious diseases. *MMBR* **77**, 173-207 (2013).

2 Bischofberger, M., Iacovache, I. & van der Goot, F. G. Pathogenic pore-forming proteins: function and host response. *Cell Host Microbe* **12**, 266-275 (2012).

3 Brown, G. D., Denning, D. W. & Levitz, S. M. Tackling human fungal infections. *Science* **336**, 647 (2012).

4 Moyes, D. L. *et al.* A biphasic innate immune MAPK response discriminates between the yeast and hyphal forms of *Candida albicans* in epithelial cells. *Cell Host Microbe* **8**, 225-235 (2010).

5 Moyes, D. L. *et al. Candida albicans* yeast and hyphae are discriminated by MAPK signaling in vaginal epithelial cells. *PLoS ONE* **6**, e26580 (2011).

6 Naglik, J. R., Richardson, J. P. & Moyes, D. L. *Candida albicans* pathogenicity and epithelial immunity. *PLoS Pathog* **10**, e1004257 (2014).

7 Moyes, D. L., Richardson, J. P. & Naglik, J. R. *Candida albicans*-epithelial interactions and pathogenicity mechanisms: scratching the surface. *Virulence* **6**, 338-346 (2015).

8 Birse, C. E., Irwin, M. Y., Fonzi, W. A. & Sypherd, P. S. Cloning and characterization of *ECE1*, a gene expressed in association with cell elongation of the dimorphic pathogen *Candida albicans*. *Infect. Immun.* **61**, 3648-3655 (1993).

9 Rohm, M. *et al.* A family of secreted pathogenesis-related proteins in *Candida albicans*. *Mol. Microbiol.* **87**, 132-151 (2013).

10 Kamai, Y., Kubota, M., Hosokawa, T., Fukuoka, T. & Filler, S. G. New model of oropharyngeal candidiasis in mice. *Antimicrob. Agents Chemother.* **45**, 3195-3197 (2001).

11 Gratacap, R. L., Rawls, J. F. & Wheeler, R. T. Mucosal candidiasis elicits NF-kappaB activation, proinflammatory gene expression and localized neutrophilia in zebrafish. *Dis. Model. Mech.* **6**, 1260-1270 (2013).

12 Brothers, K. M. *et al.* NADPH oxidase-driven phagocyte recruitment controls *Candida albicans* filamentous growth and prevents mortality. *PLoS Pathog.* **9**, e1003634 (2013).

13 Bader, O., Krauke, Y. & Hube, B. Processing of predicted substrates of fungal Kex2 proteinases from *Candida albicans*, *C. glabrata*, *Saccharomyces cerevisiae* and *Pichia pastoris*. *BMC Microbiol.* **8**, 116 (2008).

14 Liu, P., Huang, X., Zhou, R. & Berne, B. J. Observation of a dewetting transition in the collapse of the melittin tetramer. *Nature* **437**, 159-162 (2005).

15 Bechinger, B. & Salnikov, E. S. The membrane interactions of antimicrobial peptides revealed by solid-state NMR spectroscopy. *Chem. Phys. Lipids* **165**, 282-301 (2012).

16 Pieta, P., Mirza, J. & Lipkowski, J. Direct visualization of the alamethicin pore formed in a planar phospholipid matrix. *Proc. Natl. Acad. Sci. U S A* **109**, 21223-21227 (2012).

17 Oren, Z. & Shai, Y. Selective lysis of bacteria but not mammalian cells by diastereomers of melittin: structure-function study. *Biochemistry* **36**, 1826-1835 (1997).

18 Walev, I. *et al.* Delivery of proteins into living cells by reversible membrane permeabilization with streptolysin-O. *Proc. Natl. Acad. Sci. U S A* **98**, 3185-3190 (2001).

19 Zakikhany, K. *et al. In vivo* transcript profiling of *Candida albicans* identifies a gene essential for interepithelial dissemination. *Cell. Microbiol.* **9**, 2938-2954 (2007).

Figure Legends

Figure 1| *ECE1* is required for epithelial activation and mucosal *C. albicans* infection. (a) Fold change induction of LDH release after 24 h infection of TR146 epithelial cells with *C. albicans* wild type (BWP17 + CIp30), *ECE1*-deletion (*ece1*Δ/Δ) or *ECE1* re-integrant (*ece1*Δ/Δ+*ECE1*) strains (MOI = 0.1). **(b)** Induction of MKP-1 phosphorylation and c-Fos production after 2 h infection of TR146 epithelial cells with *C. albicans* wild type, *ece1*Δ/Δ or *ece1*Δ/Δ+*ECE1* strains (MOI = 10). **(c)** Fold change induction of c-Fos DNA binding after 3 h infection of TR146 epithelial cells with *C. albicans* wild type, *ece1*Δ/Δ or *ece1*Δ/Δ+*ECE1* (MOI = 10). **(d)** Induction of G-CSF production after 24 h infection of TR146 epithelial cells with *C. albicans* wild type, *ece1*Δ/Δ or *ece1*Δ/Δ+*ECE1* (MOI = 0.01). **(e-i)** PAS stained sections of tongues from OPC-infected mice 2 d post-infection. **(e)** Whole-mount (original magnification x25) and **(f)** high-power (original magnification x200) views of PAS stained tongue sections from *C. albicans* wild type infected mice. Foci of infection in **(e)** are indicated by asterisks and a high power (x200) view of one of these foci is shown in **(f)**, demonstrating the presence of invading hyphae (black arrow) and associated infiltrating inflammatory cells (blue arrow). **(g)** Whole-mount (original magnification x25) view of a PAS stained tongue section from a *C. albicans ece1*Δ/Δ-infected mouse, demonstrating no foci of infection. **(h)** Whole-mount (original magnification x25) view of a PAS stained tongue section from a *C. albicans ece1*Δ/Δ+*ECE1*-infected mouse. Foci of infection are indicated by asterisks; **(i)** High-power (x200) view of a focus of infection, demonstrating invading hyphae (black arrow) and inflammatory infiltrate (blue arrow), as seen in wild type infected mice. **(j)** Quantification of invading neutrophils at the site of infection (SOI) in a zebrafish swimbladder model after infection with *C. albicans* wild type (n = 47) or *ece1*Δ/Δ (n = 53) or PBS (vehicle, n = 40). **(k)** Quantification of damaged cells at the site of infection in a zebrafish swimbladder model after infection with *C. albicans* wild type (n = 73) or *ece1*Δ/Δ (n = 59) or PBS (vehicle, n = 63). Data are representative **(b, e-i)** or the mean **(a, c-d, j-k)** of at least three independent experiments and, where appropriate, error bars show ± SEM. * = $P < 0.05$, ** = $P < 0.01$, *** = $P < 0.001$.

Figure 2| Ece1-III$_{62-93}$ is the active region of Ece1p and is required for epithelial activation and mucosal *C. albicans* infection. **(a)** Phosphorylation of MKP-1 and production of c-Fos after 2 h stimulation of TR146 epithelial cells with the eight Ece1 peptides at 1.5 μM. **(b)** Induction of G-CSF after stimulation of TR146 epithelial cells for 24 h with varying

concentrations (70 µM - 1.5 µM) of Ece1-III$_{62-93}$. **(c)** Fold change induction of LDH release from TR146 epithelial cells after 24 h stimulation with the eight Ece1 peptides at 70 µM. **(d)** Fold change induction of c-Fos DNA binding in TR146 epithelial cells in response to 3 h stimulation with sub-lytic concentrations (15 µM - 1.5 µM) of Ece1-III$_{62-93}$. **(e)** Fold change induction of LDH release from TR146 epithelial cells after 24 h stimulation with varying concentrations (70 µM - 1.5 µM) of Ece1-III$_{62-93}$. **(f)** Phosphorylation of MKP-1 and production of c-Fos after 2 h infection of TR146 epithelial cells with *C. albicans* wild-type (BWP17 + CIp30), *ECE1*-deletion (*ece1*Δ/Δ), *ECE1* re-integrant (*ece1*Δ/Δ+*ECE1*) or Ece1-III$_{62-93}$ deletion (*ece1*Δ/Δ+*ECE1*$_{\Delta 184-279}$) strains (MOI = 10). **(g)** Fold change induction of c-Fos DNA binding in TR146 epithelial cells in response to 3 h infection with *C. albicans ece1*Δ/Δ+*ECE1* or *ece1*Δ/Δ+*ECE1*$_{\Delta 184-279}$ (MOI = 10). **(h)** Induction of G-CSF secretion after infection of TR146 epithelial cells for 24 h with *C. albicans* wild-type (BWP17 + CIp30), *ece1*Δ/Δ, *ece1*Δ/Δ+*ECE1* or *ece1*Δ/Δ+*ECE1*$_{\Delta 184-279}$ (MOI = 0.01). **(i)** Fold change induction of LDH release from TR146 epithelial cells after 24 h infection with *C. albicans ece1*Δ/Δ+*ECE1* or *ece1*Δ/Δ+*ECE1*$_{\Delta 184-279}$ (MOI = 0.01). **(j-l)** PAS stained tongue sections from OPC-infected mice after 2 d infection with **(j, k)** *C. albicans ece1*Δ/Δ+*ECE1* (x25 and x200) or **(l)** *ece1*Δ/Δ+*ECE1*$_{\Delta 184-279}$. Invading hyphae (black arrows) and infiltrating inflammatory cells (blue arrow) are shown. **(m)** Quantification of damaged cells at the site of infection in a zebrafish swimbladder model after infection with *C. albicans ece1*Δ/Δ+*ECE1* (n = 44) or *ece1*Δ/Δ+*ECE1*$_{\Delta 184-279}$ (n = 58) or PBS (vehicle, n = 58). **(n-o)** Direct damage induced by Ece1-III$_{62-93}$ in a zebrafish swimbladder model. **(n)** Quantification of damaged cells in zebrafish swimbladders after stimulation with 9 ng/fish (n = 51) or 1.25 ng/fish (n = 56) of Ece1-III$_{62-93}$. DMSO was the vehicle control (40% DMSO, n = 54 and 5% DMSO, n = 55). **(o)** Co-localization of adherens junctions (α-catenin-citrine) with Ece1-III$_{62-93}$-damaged epithelial cells (Sytox Orange-positive cells) in the swimbladder by intravital imaging of zebrafish. Data are representative **(a, f, j-l, o)** or the mean **(b-e, g-i, m-n)** of at least three independent experiments **(a-m)** or ten fish **(n-o)** and, where appropriate, error bars show ± SEM. * = $P < 0.05$, ** = $P < 0.01$, *** = $P < 0.001$ (compared with vehicle control).

Figure 3| Ece1-III$_{62-93}$ functions as a cytolytic peptide toxin. **(a)** Raw time-dependent changes in conductance of tethered lipid membranes. Strong permeabilization by Ece1-III$_{62-93}$ of pure DOPC membranes and DOPC membranes containing 10% cholesterol. Peptide concentrations shown on panel. **(b)** Evoked inward current at a membrane potential of -60 mV in TR146 epithelial cell membranes after the addition of Ece1-III$_{62-93}$ (70 µM - 1.5 µM) or

ionomycin (10 µM, positive control), showing both individual (representative) and cumulative changes (bar chart - number of cells analysed below each bar). Water was the vehicle control. **(c)** Changes in intracellular calcium levels in TR146 epithelial cells over time after stimulation with Ece1-III$_{62\text{-}93}$ wild type (Ece1-III$_{62\text{-}93KR}$) or Ece1-III$_{62\text{-}93}$ AA C-terminal substitution (Ece1-III$_{62\text{-}93AA}$) at different concentrations (70 µM - 1.5 µM). **(d)** Raw time-dependent changes in conductance of tethered DOPC membranes, showing strong permeabilization by Ece1-III$_{62\text{-}93KR}$ but extremely weak permeabilization by Ece1-III$_{62\text{-}93AA}$. Peptide concentrations shown on panel. **(e)** Fold change induction of LDH release from TR146 epithelial cells after 24 h stimulation with Ece1-III$_{62\text{-}93KR}$ or Ece1-III$_{62\text{-}93AA}$ at varying concentrations (70 µM - 1.5 µM). **(f)** Phosphorylation of MKP-1 and production of c-Fos after 2 h treatment of TR146 epithelial cells with Ece1-III$_{62\text{-}93KR}$ or Ece1-III$_{62\text{-}93AA}$ at varying concentrations (15 µM - 1.5 µM). Induction of **(g)** G-CSF and **(h)** IL-1α secretion from TR146 epithelial cells after 24 h stimulation with Ece1-III$_{62\text{-}93KR}$ or Ece1-III$_{62\text{-}93AA}$ at varying concentrations (70 µM - 1.5 µM). Data shown are representative **(a, d, f)** or mean **(b-c, e, g-h)** of at least three independent experiments and, where appropriate, error bars show ± SEM. * = $P < 0.05$, ** = $P < 0.01$, *** = $P < 0.001$.

Figure 4| Ece1-III$_{62\text{-}92K}$ functions as a cytolytic peptide toxin that activates and damages epithelial cells. **(a)** Phosphorylation of MKP-1 and production of c-Fos after 2 h stimulation, and **(b)** Induction of G-CSF and IL-1-α after 24 h stimulation, and **(c)** Fold change induction of LDH after 24 h stimulation of TR146 epithelial cells with varying concentrations (70 µM - 1.5 µM) of Ece1-III$_{62\text{-}92K}$. **(d)** Förster resonance energy transfer (FRET) experiments showing the intercalation of Ece1-III$_{62\text{-}92K}$ into lipid liposomes (10 µM) composed of DOPC in the absence or presence of cholesterol. Peptide titration of Ece1-III$_{62\text{-}92K}$ to liposomes showed similar intercalation for both pure DOPC and DOPC containing host cholesterol. **(e)** Average peptide concentration-dependent changes in conductance of tethered lipid membranes. Strong permeabilization by Ece1-III$_{62\text{-}92K}$ of pure DOPC membranes, which was increased in the presence of cholesterol. **(f)** Ece1-III$_{62\text{-}92K}$ induced the permeabilization of planar lipid membranes composed of DOPC. The graph shows heterogeneous and transient lesions leading finally to a rupture of the membrane. Ece1-III$_{62\text{-}92K}$ concentration was 4 µM. **(g)** Changes in intracellular calcium levels in a TR146 epithelial cells over time after stimulation with Ece1-III$_{62\text{-}92K}$ at different concentrations (70 µM - 1.5 µM). Data shown are representative **(a, d, f)** or mean **(b-c, e, g)** of at least three independent experiments and, where appropriate, error bars show ± SEM. * = $P < 0.05$, ** = $P < 0.01$, *** = $P < 0.001$.

Extended Data Figure legends

Extended Data Figure 1: *C. albicans ECE1* expression and phenotypic effects of *ECE1* gene deletion. **(a)** Relative expression (vs t = 0) of *ECE1* in *C. albicans* wild type over time after addition of yeast cells to TR146 epithelial cells as measured by RT-qPCR. **(b)** Imaging confirmation of *ECE1* expression over time within *C. albicans* wild type. *C. albicans* cells expressing GFP under the control of the *ECE1* 5' intragenic region, containing the *ECE1* promoter, were grown on TR146 epithelial cells and stained with calcofluor white (CFW, post-permeabilization) to show cell wall chitin and Alexa-Fluor-647-labelled concanavalin A (ConA, pre-permeabilization) to show carbohydrates. A composite image showing CFW, ConA, GFP and the brightfield (BF) image is shown. **(c)** Scanning electron micrographs (top panels, 5 h) and light microscopy (bottom panels, 24 h) showing no gross abnormalities in hypha formation between *C. albicans* wild type (BWP17+CIp30), *ECE1*-deletion (*ece1*Δ/Δ) and *ECE1* re-integrant (*ece1*Δ/Δ+*ECE1*) strains after infection of TR146 epithelial cells. **(d)** No difference in adhesion of *C. albicans* wild type, *ece1*Δ/Δ and *ece1*Δ/Δ+*ECE1* strains to TR146 epithelial cells after 60 min. **(e)** No difference in invasion of *C. albicans* wild type, *ece1*Δ/Δ and *ece1*Δ/Δ+*ECE1* strains into TR146 epithelial cells after 3 h. **(f)** Fluorescence staining of *C. albicans* wild type and *ece1*Δ/Δ hyphae invading through TR146 epithelial cells. Fungal cells are stained with calcofluor white (CFW, post-permeabilization) and Alexa-Fluor-647-labelled concanavalin A (ConA, pre-permeabilization) to show cell wall chitin and carbohydrates, respectively, and to distinguish between invading hyphae (only stained after permeabilization) and non-invading hyphae (stained both pre- and post-permeabilization). Levels of chitin and β-glucan are comparable in both strains. White arrows indicate invasion into epithelial cells. Data shown are representative **(b, c, f)** or the mean **(a, d, e)** of at least three independent experiments.

Extended Data Figure 2: *C. albicans* Ece1p is critical for mucosal virulence *in vivo*. (a) Fungal burdens recovered from the tongues of mice infected with *C. albicans* wild type (BWP17+CIp30) (n = 13), *ECE1*-deletion (*ece1Δ/Δ*) (n = 20) and *ECE1* re-integrant (*ece1Δ/Δ+ECE1*) (n = 24) strains after 2 day oropharyngeal infection. The number of animals in each group is indicated above the bar. **(b)** Average percentage of the entire tongue epithelium length infected in different groups of mice infected with the different *C. albicans* strains. **(c)**

Confocal imaging of 4 day post-fertilization (dpf) *mpo-gfp* transgenic zebrafish swimbladders infected with *C. albicans* wild type (BWP17+CIp30+*dTomato*), *ECE1*-deletion (*ece1Δ/Δ+dTomato*) and *ECE1* re-integrant (*ece1Δ/Δ+ECE1+dTomato*) strains for 24 h. *C. albicans* cells appear red whilst neutrophils appear green. Red dots outline the swimbladder. Images are composites of maximum projections in the red and green channels (25 slices each, approximately 100 μm depth) with (left) or without (right) a single slice in the DIC channel overlay. Scale bars represent 100 μm. **(d)** Confocal imaging of 4 dpf zebrafish swimbladders infected with *C. albicans* wild type (BWP17+CIp30+*dTomato*), *ECE1*-deletion (*ece1Δ/Δ+dTomato*) and *ECE1* re-integrant (*ece1Δ/Δ+ECE1+dTomato*) strains for 24 h stained with the fluorescent exclusion dye Sytox Green. *C. albicans* cells appear red and damaged epithelial cells appear green. White dots outline the pronephros and red dots outline the swimbladder. Images are composites of maximum projections in the red and green channels (25 slices each, approximately 100 μm depth) with (left) or without (right) a single slice in the DIC channel overlay. High magnification images of the white boxes are shown. Scale bars represent 100 μm (low magnification) and 30 μm (high magnification). Data shown are the mean **(a)** or representative **(b, c)** of at least three independent experiments. Where appropriate, error bars show ± SEM. *** = $P < 0.001$.

Extended Data Figure 3: Ece1-III$_{62-93}$ is the active region of Ece1p. (a) Amino acid sequence of Ece1p and a schematic of the protein, indicating the signal peptide (SP), lysine-arginine motifs (KR) at the C-terminus of each peptide, and the processed peptides (Ece1-I-VIII) produced by Kex2p cleavage. **(b)** Amino acid sequences of the processed peptides (Ece1-I-VIII) produced by Kex2p cleavage. Induction of **(c)** GM-CSF, **(d)** IL-1α and **(e)** IL-6 secreted after stimulation of TR146 epithelial cells for 24 h with varying concentrations of Ece1-III$_{62-93}$ (70 μM - 1.5 μM). **(f)** Phosphorylation of MKP-1 and c-Fos production after 2 h treatment of TR146 epithelial cells with 15 μM of Ece1-III$_{62-85}$ (hydrophobic region), Ece1-III$_{86-93}$ (hydrophillic region), Ece1-III$_{62-85}$ and Ece1-III$_{86-93}$ together, or Ece1-III$_{62-93}$ alone. **(g)** Induction of G-CSF secretion after 24 h treatment of TR146 epithelial cells with 15 μM of Ece1-III$_{62-85}$, Ece1-III$_{86-93}$, Ece1-III$_{62-85}$ and Ece1-III$_{86-93}$ together, or Ece1-III$_{62-93}$ alone. **(h)** Fold change induction of LDH release after 24 h treatment of TR146 epithelial cells with 70 μM of Ece1-III$_{62-85}$, Ece1-III$_{86-93}$, Ece1-III$_{62-85}$ and Ece1-III$_{86-93}$ together, or Ece1-III$_{62-93}$ alone. Data shown are representative **(f)** or the mean **(c-e, g-h)** of at least three independent experiments. Where appropriate, error bars show ± SEM. * = $P < 0.05$, ** = $P < 0.01$, *** = $P < 0.001$ (compared with vehicle control).

Extended Data Figure 4: Ece1-III$_{62-93}$ is required for *C. albicans* mucosal infection. (a) Fungal burdens recovered from the tongues of mice infected with *C. albicans* wild type (BWP17+CIp30) (n = 13), *ECE1*-deletion (*ece1Δ/Δ*) (n = 20), *ECE1* re-integrant (*ece1Δ/Δ+ECE1*) (n = 24) and Ece1-III$_{62-93}$ deletion (*ece1Δ/Δ+ECE1$_{Δ184-279}$*) (n = 10) strains after 2 day oropharyngeal infection. **(b)** Average percentage of the entire tongue epithelium length infected in different groups of mice infected with the different *C. albicans* strains. **(c)** Confocal imaging of 4 dpf zebrafish swimbladders infected with *C. albicans* Ece1-III$_{62-93}$ deletion (*ece1Δ/Δ+ECE1$_{Δ184-279}$+dTomato*) and *ECE1* re-integrant (*ece1Δ/Δ+ECE1+dTomato*) strains for 24 h stained with the fluorescent exclusion dye Sytox Green. *C. albicans* cells appear red and damaged cells appear green. White dots outline the pronephros and red dots outline the swimbladder. Images are composites of maximum projections in the red and green channels (25 slices each, approximately 100 µm depth) with (left) or without (right) a single slice in the DIC channel overlay. Scale bars represent 100 µm. Data shown are the mean **(a)** or representative **(b, c)** of at least three independent experiments. Where appropriate, error bars show ± SEM. ** = $P < 0.01$, *** = $P < 0.001$.

Extended Data Figure 5: Ece1-III$_{62-93}$ is a cytolytic α-helical peptide. (a) Circular dichroism spectra showing the α-helical conformation of Ece1-III$_{62-93}$ in buffer (100 mM KCl, 5 mM HEPES, pH 7). Increasing the temperature from 25ºC to 40ºC did not affect the stability of the α-helical structure. **(b)** Diagram to illustrate the amphipathic nature of Ece1-III$_{62-93}$ (residues 62-78, left panel; residues 79-93, right panel). Residues with hydrophobic or polar/charged side chains are displayed with a blue and white background, respectively. Modified from output generated in PEPWHEEL (http://emboss.bioinformatics.nl/cgi-bin/emboss/pepwheel). **(c)** Förster resonance energy transfer (FRET) experiments show the intercalation of Ece1-III$_{62-93}$ into lipid liposomes (10 µM) composed of DOPC in the absence or presence of cholesterol. Peptide titration of Ece1-III$_{62-93}$ to liposomes showed slightly enhanced intercalation for pure DOPC. **(d)** Ece1-III$_{62-93}$ induced the permeabilization of planar lipid membranes composed of DOPC. The graph shows heterogeneous and transient lesions leading finally to a rupture of the membrane. Ece1-III$_{62-93}$ concentration was 0.125 µM.

Extended Data Figure 6: Schematic of the role of Ece1-III in *C. albicans* infection of epithelial cells. During early stage infection of the mucosal surface by *C. albicans*, Ece1-III (red α-helix) is secreted into the invasion pocket created by the invading hypha **(a)**. Sub-lytic

concentrations of Ece1-III trigger epithelial signal transduction through MAPK, p38/MKP-1 and c-Fos **(b)** resulting in the production of immune regulatory cytokines **(c)**. As the severity of the infection increases, Ece1-III accumulates **(d)** and once lytic concentrations are reached, causes membrane damage and the release of lactate dehydrogenase from the host epithelium **(e)**, concomitant with calcium influx **(f)**. Epithelial signal transduction is maintained **(g)** and additionally induces the release of damage associated cytokines, such as IL-1α **(h)**. Ece1-III may also have activity on the epithelial surface outside of the invasion pocket and on neighbouring cells not in contact with hyphae if Ece1-III is produced in sufficient concentrations.

METHODS

Cell lines, reagents and *Candida* strains

Experiments were carried out using the TR146 buccal epithelial squamous cell carcinoma line[20] grown in Dulbecco's Modified Eagle's Medium (DMEM, Sigma-Aldrich) supplemented with 10% fetal bovine serum (FBS) and 1% penicillin-streptomycin. Prior to stimulation, confluent TR146 epithelial cells were serum-starved overnight, and all experiments were carried out in serum-free DMEM. *C. albicans* wild type strains included the autotrophic strain BWP17+CIp30[21] and the parental strain SC5314[22]. Other *C. albicans* strains used and their sources are listed in **Extended Data Tables 1 and 2**. *C. albicans* cultures were grown in YPD medium (1% yeast extract, 2% peptone, 2% dextrose) at 30°C overnight. Cultures were washed in sterile PBS and adjusted to the required cell density. Antibodies to phospho-MKP1 and c-Fos were from Cell Signalling Technologies (New England Biolabs UK), mouse anti-human α-actin was from Millipore (UK), and goat anti-mouse and anti-rabbit horseradish peroxidase (HRP)-conjugated antibodies were from Jackson Immunologicals Ltd (Stratech Scientific, UK). Ece1p peptides were synthesised commercially (Proteogenix (France) or PeptideSynthetics (UK).

Generation of *C. albicans ECE1* mutant strains

ECE1 deletion was performed as previously described[23]. Deletion cassettes were generated by PCR[24]. Primers ECE1-FG and ECE1-RG were used to amplify pFA-HIS1 and pFA-ARG4 -based markers. *C. albicans* BWP17[25], was sequentially transformed[26] with the *ECE1*-HIS1 and *ECE1*-ARG4 deletion cassettes and then transformed with CIp10[27], yielding the *ece1*Δ/Δ deletion strain. For complementation, the *ECE1* gene plus upstream and downstream intergenic regions were amplified with primers ECE1-RecF3k and ECE1-RecR and cloned into plasmid CIp10[8] at *Mlu*I and *Sal*I sites. This plasmid was transformed into the uridine auxotrophic *ece1*Δ/Δ strain, yielding the *ece1*Δ/Δ+*ECE1* complemented strain. For generation of the *ece1*Δ/Δ+*ECE1*$_{\Delta 184\text{-}279}$ strain, the CIp10-*ECE1* was amplified with primers Pep3-F1 and Pep3-R1[27], yielding the CIp10+*ECE1*$_{\Delta 184\text{-}279}$ plasmid. This plasmid was transformed into the uridine auxotrophic *ece1*Δ/Δ strain, yielding the *ece1*Δ/Δ+*ECE1*$_{\Delta 184\text{-}279}$ strain. All integrations were confirmed by PCR/sequencing and at least two independent isogenic transformants were created to confirm results. *KEX1* deletion was performed exactly as the *ECE1* deletion but using primers KEX1-FG and KEX1-RG for creating the deletion cassette. Fluorescent strains of *ece1*Δ/Δ and BWP17 were constructed as previously described[28]. Briefly, the *ece1*Δ/Δ and

BWP17 strains were transformed with the pENO1-dTom-NATr plasmid. Primers used to clone and construct the *ECE1* genes and intragenic regions are listed in **Extended Data Table 3**. Strains are listed in **Extended Data Table 2.**

Construction of *C. albicans ECE1* promoter-GFP strain

ECE1 promoter (primers 5'*ECE1*prom-NarI / 3'*ECE1*prom-XhoI) and terminator (5'*ECE1*term-SacII / 5'*ECE1*term-SacI) were amplified and cloned into pADH1-GFP. Resulting pSK-p*ECE1*-GFP was verified by sequencing. *C. albicans* SC5314 was transformed with the *pECE1-GFP* transformation cassette[26]. Resistance to nourseothricin was used as selective marker and correct integration of GFP into the *ECE1* locus was verified by PCR. Primers for cloning and validation are listed in **Extended Data Table 3**. Strains are listed in **Extended Data Table 2**.

RNA isolation and real-time PCR analysis

C. albicans cells grown on TR146 epithelial cells were collected into RNA pure (PeqLab), centrifuged and the pellet resuspended in 400 µl AE buffer (50 mM Na-acetate pH 5.3, 10 mM EDTA, 1% SDS). Samples were vortexed (30 s), and an equal volume of phenol/chloroform/isoamyl alcohol (25:24:1) was added and incubated for 5 min (65°C) before subjected to 2x freeze-thawing. Lysates were clarified by centrifugation and the RNA precipitated with isopropyl alcohol/0.3 M sodium acetate by incubating for 1 h at -20°C. Precipitated pellets were washed (2x 1 ml 70% ice-cold ethanol), resuspended in DEPC-treated water and stored at -80°C. RNA integrity and concentration was confirmed using a Bioanalyzer (Agilent). RNA (500 ng) was treated with DNase (Epicenter) and cDNA synthesized using Reverse Transcriptase Superscript III (Invitrogen). cDNA samples were used for qPCR with EVAgreen mix (Bio&Sell). Primers (ACT1-F and ACT1-R for actin, ECE1-F and ECE1-R for *ECE1* - **Extended Data Table 3**) were used at a final concentration of 500 nM. qPCR amplifications were performed using a Biorad CFX96 thermocycler. Data was evaluated using Bio-Rad CFX Manager 3.1 (Bio-Rad) with *ACT1* as the reference gene and t_0 as the control sample.

Western blotting

TR146 cells were lysed using a modified RIPA lysis buffer (50 mM Tris-HCl pH 7.4, 150 mM NaCl, 1 mM EDTA, 1% Triton X-100, 1% sodium deoxycholate, 0.1% SDS) containing protease (Sigma-Aldrich) and phosphatase (Perbio Science) inhibitors[29], left on ice (30 min)

and then clarified (10 min) in a refrigerated microfuge. Lysate total protein content was determined using the BCA protein quantitation kit (Perbio Science). 20 µg of total protein was separated on 12% SDS-PAGE gels before transfer to nitrocellulose membranes (GE Healthcare). After probing with primary (1:1000) and secondary (1:10,000) antibodies, membranes were developed using Immobilon chemiluminescent substrate (Millipore) and exposed to X-Ray film (Fuji film). Human α-actin was used as a loading control.

Transcription factor DNA binding assay

DNA binding activity of transcription factors was assessed using the TransAM transcription factor ELISA system (Active Motif) as previously described[29,30]. Serum-starved TR146 epithelial cells were treated for 3 h before being differentially lysed to recover nuclear proteins using a nuclear protein extraction kit (Active Motif) according to the manufacturer's protocol. Protein concentration was determined (BCA protein quantitation kit (Perbio Science)) and 5 µg of nuclear extract was assayed in the TransAM system according to the manufacturer's protocol. Data was expressed as fold-change in A_{450nm} relative to resting cells.

Cytokine determination

Cytokine levels in cell culture supernatants were determined using the Performance magnetic Fluorokine MAP cytokine multiplex kit (Bio-techne) and a Bioplex 200 machine. The data were analysed using Bioplex Manager 6.1 software to determine analyte concentrations.

Cell damage assay

Following incubation, culture supernatant was collected and assayed for lactate dehydrogenase (LDH) activity using the Cytox 96 Non-Radioactive Cytotoxicity Assay kit (Promega) according to the manufacturer's instructions. Recombinant porcine LDH (Sigma-Aldrich) was used to generate a standard curve.

Epithelial adhesion assay

Quantification of *C. albicans* adherence to TR146 epithelial cells was performed as described previously[31]. Briefly, TR146 cells were grown to confluence on glass coverslips for 48 h in tissue culture plates in DMEM medium. *C. albicans* yeast cells (2×10^5) were added into 1 ml serum-free DMEM, incubated for 60 min (37°C/5% CO_2) and non-adherent *C. albicans* cells removed by aspiration. Following washing (3x 1 ml PBS), cells were fixed with 4%

paraformaldehyde (Roth) and adherent *C. albicans* cells stained with Calcofluor White and quantified using fluorescence microscopy. The number of adherent cells was determined by counting 100 high power fields of 200 µm × 200 µm size. Exact total cell numbers were calculated based on the quantified areas and the total size of the cover slip.

Epithelial invasion assay

C. albicans invasion of epithelial cells was determined as described previously[31]. Briefly, TR146 epithelial cells were grown to confluence on glass coverslips for 48 h and then infected with *C. albicans* yeast cells (1×10^5), for 3 h in a humidified incubator (37°C/5% CO_2). Following washing (3x PBS), the cells were fixed with 4% paraformaldehyde. All surface adherent fungal cells were stained for 1 h with a rabbit anti-*Candida* antibody and subsequently with a goat anti-rabbit-Alexa Fluor 488 antibody. After rinsing with PBS, epithelial cells were permeabilised (0.1% Triton X-100 in PBS for 15 min) and fungal cells (invading and non-invading) were stained with Calcofluor White. Following rinsing with water, coverslips were visualized using fluorescence microscopy. The percentage of invading *C. albicans* cells was determined by dividing the number of (partially) internalized cells by the total number of adherent cells. At least 100 fungal cells were counted on each coverslip.

Imaging of *C. albicans* growth and invasion of epithelial cells

TR146 cells (10^5/ml) seeded on glass coverslips in DMEM/10% FBS were infected with *C. albicans* (2.5×10^4 cfu/ml) in DMEM and incubated for 6 h (37°C/5% CO_2). Cells were washed with PBS, fixed overnight (4°C in 4% paraformaldehyde) and stained with Concanavalin A-Alexa Fluor 647 in PBS (10 µg/ml) for 45 min at room temperature in the dark with gentle shaking (70 rpm) to stain the fungal cell wall. Epithelial cells were permeabilised with 0.1% Triton X-100 for 15 min at 37°C in the dark, then washed and stained with 10 µg/ml Calcofluor White (0.1 M Tris-HCl pH 9.5) for 20 min at room temperature in the dark with gentle shaking. Cells were rinsed in water and mounted on slides with 6 µl of ProLong Gold antifade reagent, before air drying for 2 h in the dark. Fluorescence microscopy was performed on a Zeiss Axio Observer Z1 microscope, and 5 phase images were taken per picture.

Scanning Electron Microscopy

For scanning electron microscopy (SEM) analysis, TR146 cells were grown to confluence on Transwell inserts (Greiner) and serum starved overnight in serum-free DMEM. After 5 h of *C.*

albicans incubation on epithelial cells at an MOI of 0.01, cell media was removed and samples were fixed overnight at 4ºC with 2.5% (v/v) glutaraldehyde in 0.05 M HEPES buffer (pH 7.2) and post-fixed in 1% (w/v) osmium tetroxide for 1 h at room temperature. After washing, samples were dehydrated through a graded ethanol series before being critical point dried (Polaron E3000, Quorum Technologies Ltd). Dried samples were mounted using carbon double side sticky discs (TAAB) on aluminium pins (TAAB) and gold coated in an Emitech K550X sputter coater (Quorum Technologies Ltd). Samples were examined and images recorded using a FEI Quanta 200 field emission scanning electron microscope operated at 3.5 kV in high vacuum mode.

Zebrafish swimbladder mucosal infection model

Ten to twenty zebrafish per group per experiment ('n' in each figure legend) were maintained at 33°C in E3 + PTU and used as previously described[28]. Briefly, 4 day post-fertilization (dpf) larvae were treated with 20 μg/ml dexamethasone dissolved in 0.1% DMSO 1 h prior to infection and thereafter. For tissue damage and neutrophil recruitment, individual AB or *mpo:GFP* fish (respectively) were injected into the swimbladder with 4 nl of PBS with/without 25-40 *C. albicans* yeast cells of *ece1*Δ/Δ-*dTomato* or BWP17-*dTomato*. For tissue damage, 1 nl of Sytox green (0.05 mM in 1% DMSO) was injected at 20 h post-infection into the swimbladder and fish were imaged by confocal microscopy at 24 h post-infection. For neutrophil recruitment, fish were imaged at 24 h post-injection. For synthetic peptide damage, AB or α-catenin:citrine[32] fish were injected with 2 nl of peptide (9 ng or 1.25 ng per fish) or vehicle (40% DMSO or 5% DMSO) + SytoxGreen (0.05 mM in 1% DMSO) or SytoxOrange (0.5 mM in 10% DMSO) and the fish imaged by confocal microscopy 4 h later. Numbers of neutrophils and damaged cells observed were counted and tabulated for each fish.

Zebrafish swimbladder fluorescence microscopy

Live zebrafish imaging was carried out as previously described[28]. Briefly, fish were anesthetized in Tris-buffered Tricaine (200 μg/ml, Western Chemicals) and further immobilized in a solution of 0.4% low-melting-point agarose (LMA, Lonza) in E3 + Tricaine in a 96-well plate glass-bottom imaging dish (Greiner Bio-On). Confocal imaging was carried out using an Olympus IX-81 inverted microscope with an FV-1000 laser scanning confocal system (Olympus). Images were collected and processed using Fluoview (Olympus) and Photoshop (Adobe Systems Inc.). Panels are either a single slice for the differential interference contrast channel (DIC) with maximum projection overlays of fluorescence image channels

(red-green), or maximum projection overlays of fluorescence channels. The number of slices for each maximum projection is specified in the legend of individual figures.

Murine oropharyngeal candidiasis model

A previously described murine model of oropharyngeal candidiasis using female Balb/c mice[33] was modified for investigating early infection events. Briefly, mice were treated sub-cutaneously with 3 mg/mouse (in 200 µl PBS with 0.5% Tween 80) of cortisone acetate on days -1 and 1 post-infection. On day 0, mice were sedated for ~75 min with an intra-peritoneal injection of 110 mg/kg ketamine and 8 mg/kg xylazine, and a swab soaked in a 10^7 cfu/ml *C. albicans* yeast culture in sterile saline was placed sub-lingually for 75 min. After 2 days, mice were sacrificed, the tongue excised and divided longitudinally in half. One half was weighed, homogenized and cultured to derive quantitative *Candida* counts. The other half was processed for histopathology and immunohistochemistry.

Immunohistochemistry of murine tissue

C. albicans infected murine tongues were fixed in 10% (v/v) formal-saline before being embedded and processed in paraffin wax using standard protocols. For each tongue, 5 µm sections were prepared using a Leica RM2055 microtome and silane coated slides. Sections were dewaxed using xylene, before *C. albicans* and infiltrating inflammatory cells were visualised by staining using Periodic Acid-Schiff (PAS) stain and counterstaining with haematoxylin. Sections were then examined by light microscopy.

Whole cell patch clamp

TR146 epithelial cells were grown in 35 mm petri dishes (Nunc) for 48 h before recordings at low cell density (10-30% confluence). Cells were superfused with a modified Krebs solution (120 mM NaCl, 3 mM KCl, 2.5 mM $CaCl_2$, 1.2 mM $MgCl_2$, 22.6 mM $NaHCO_2$, 11.1 mM glucose, 5 mM HEPES pH 7.4). Isolated cells were recorded at room temperature (21-23^{o}C) in whole cell mode using microelectrodes (5-7 MΩ) containing 90 mM potassium acetate, 20 mM KCl, 40 mM HEPES, 3 mM EGTA, 3 mM $MgCl_2$, 1 mM $CaCl_2$ (free Ca^{2+} 40 nM), pH 7.4. Cells were voltage clamped at -60 mV using an Axopatch 200A amplifier (Axon Instruments) and current/voltage curves were generated by 1 s steps between -100 to + 50 mV. Treatments were applied to the superfusate to produce the final required concentration, with vehicle controls similarly applied. Data was recorded using Clampex software (PClamp 6, Axon Instrument) and analyzed with Clampfit 10.

Calcium flux

TR146 cells were grown in a 96-well plate overnight until confluent. The medium was removed and 50 µl of a Fura-2 solution (5 µl Fura-2 (Life Technologies)(2.5 mM in 50% Pluronic F-127 (Life technologies):50% DMSO), 5 µl probenecid (Sigma) in 5 ml saline solution (NaCl (140 mM), KCl (5 mM), $MgCl_2$ (1 mM), $CaCl_2$ (2 mM), Glucose (10 mM) and HEPES (10 mM), adjusted to pH 7.4)) was added and the plate incubated for 1 h at 37°C/5% CO_2. The Fura-2 solution was replaced with 50 µl saline solution and baseline fluorescence readings (excitation 340 nm/emission 520nm) taken for 10 min using a FlexStation 3 (Molecular Devices). Ece1 peptides were added at different concentrations and readings immediately taken for up to 3 h. The data was analyzed using Softmax Pro software to determine calcium present in the cell cytosol and expressed as the ratio between excitation and emission spectra.

Impedance spectroscopy of tethered bilayer lipid membranes (tBLMs)

tBLMs with 10% tethering lipids and 90% spacer lipids (T10 slides) were formed using the solvent exchange technique[34,35] according to the manufacturer's instructions (SDx Tethered Membranes Pty Ltd, Sydney, Australia). Briefly, 8 µl of 3 mM lipid solutions in ethanol were added, incubated for 2 min and then 93.4 µl buffer (100 mM KCl, 5 mM HEPES, pH 7.0) was added. After rinsing 3x with 100 µl buffer the conductance and capacitance of the membranes were measured for 20 min before injection of Ece1 peptides at different concentrations. All experiments were performed at room temperature. Signals were measured using the tethaPod (SDx Tethered Membranes Pty Ltd, Sydney, Australia).

FRET intercalation experiments

Intercalation of Ece1 peptides into phospholipid liposomes was determined by FRET spectroscopy applied as a probe-dilution assay[36]. Phospholipids mixed with each 1% (mol/mol) of the donor dye NBD-phosphatidylethanolamine (NBD-PE) and of the acceptor dye rhodamine-PE, were dissolved in chloroform, dried, solubilized in 1 ml buffer (100 mM KCl, 5 mM HEPES, pH 7.0) by vortexing, sonicated with a titan tip (30 W, Branson sonifier, cell disruptor B15), and subjected to three cycles of heating to 60°C and cooling down to 4°C, each for 30 min. Lipid samples were stored at 4°C for at least 12 h before use. Ece1 peptide was added to liposomes and intercalation was monitored as the increase of the quotient between the donor fluorescence intensity I_D at 531 nm and the acceptor intensity I_A at 593 nm (FRET signal) independent of time.

Circular Dichroism spectroscopy

CD measurements were performed using a Jasco J-720 spectropolarimeter (Japan Spectroscopic Co., Japan), calibrated as described previously[37]. CD spectra represent the average of four scans obtained by collecting data at 1 nm intervals with a bandwidth of 2 nm. The measurements were performed in 100 mM KCl, 5 mM HEPES, pH 7.0 at 25°C and 40°C in a 1.0 mm quartz cuvette. The Ece1-III concentration was 15 µM.

Planar lipid bilayers

Planar lipid bilayers were prepared using the Montal-Mueller technique[38] as described previously[39]. All measurements were performed in 5 mM HEPES, 100 mM KCl, pH 7.0 (specific electrical conductivity 17.2 mS/cm) at 37°C.

Hyphal secretome preparation for LC-MS/MS analysis

Candida strains were cultured for 18 h in hyphae inducing conditions (YNB medium containing 2% sucrose, 75 mM MOPSO buffer pH 7.2, 5 mM N-acetyl-D-glucosamine, 37°C). Hyphal supernatants were collected by filtering through a 0.2 µm PES filter, and peptides were enriched by Solid Phase Extraction (SPE) using first C4 and subsequently C18 columns on the C4 flowthrough. After drying in a vacuum centrifuge, samples were resolubilised in loading solution (0.2% formic acid in 71:27:2 ACN/H_2O/DMSO (v/v/v)) and filtered through a 10 kDa MWCO filter. The filtrate was transferred into HPLC vials and injected into the LC-MS/MS system. LC-MS/MS analysis was carried out on an Ultimate 3000 nano RSLC system coupled to a QExactive Plus mass spectrometer (ThermoFisher Scientific). Peptide separation was performed based on a direct injection setup without peptide trapping using an Accucore C4 column as stationary phase and a column oven temperature of 50°C. The binary mobile phase consisting of A) 0.2% (v/v) formic acid in 95:5 H_2O/DMSO (v/v) and B) 0.2% (v/v) formic acid in 85:10:5 ACN/H_2O/DMSO (v/v/v) was applied for a 60 min gradient elution: 0-1.5 min at 60% B, 35-45 min at 96% B, 45.1-60 min at 60% B. The Nanospray Flex Ion Source (ThermoFisher Scientific) provided with a stainless steel emitter was used to generate positively charged ions at 2.2 kV spray voltage. Precursor ions were measured in full scan mode within a mass range of m/z 300-1600 at a resolution of 70k FWHM using a maximum injection time of 120 ms and an automatic gain control target of 1e6. For data-dependent acquisition, up to 10 most abundant precursor ions per scan cycle with an assigned charge state of z = 2-6 were selected in the quadrupole for further fragmentation using an isolation width

of m/z 2.0. Fragment ions were generated in the HCD cell at a normalised collision energy of 30 V using nitrogen gas. Dynamic exclusion of precursor ions was set to 20 s. Fragment ions were monitored at a resolution of 17.5k (FWHM) using a maximum injection time of 120 ms and an AGC target of 2e5.

Protein database search

Thermo raw files were processed by the Proteome Discoverer (PD) software v1.4.0.288 (Thermo). Tandem mass spectra were searched against the Candida Genome Database (http://www.candidagenome.org/download/sequence/C_albicans_SC5314/Assembly22/current/C_albicans_SC5314_A22_current_orf_trans_all.fasta.gz; status: 2015/05/03) using the Sequest HT search algorithm. Mass spectra were searched for both unspecific cleavages (no enzyme) and tryptic peptides with up to 4 missed cleavages. The precursor mass tolerance was set to 10 ppm and the fragment mass tolerance to 0.02 Da. Target Decoy PSM Validator node and a reverse decoy database was used for (qvalue) validation of the peptide spectral matches (PSMs) using a strict target false discovery (FDR) rate of < 1%. Furthermore, we used the Score versus Charge State function of the Sequest engine to filter out insignificant peptide hits (xcorr of 2.0 for z=2, 2.25 for z=3, 2.5 for z=4, 2.75 for z=5, 3.0 for z=6). At least two unique peptides per protein were required for positive protein hits.

Statistics

TransAM and patch clamp data were analyzed using a paired t-test whilst cytokines, LDH and calcium influx data were analyzed using ANOVA. Murine *in vivo* $\text{Log}_{(10)}$ cfu/g data was analyzed using the Mann-Whitney test. Zebrafish data was analyzed using the Kruskal-Wallis test with Dunn's multiple comparison correction. In all cases, $P < 0.05$ was taken to be significant.

References

20 Rupniak, H. T. *et al.* Characteristics of four new human cell lines derived from squamous cell carcinomas of the head and neck. *J. Nat. Cancer Instit.* **75**, 621-635 (1985).

21 Mayer, F. L. *et al.* The novel *Candida albicans* transporter Dur31 is a multi-stage pathogenicity factor. *PLoS Pathogen.* **8**, e1002592 (2012).

22 Gillum, A. M., Tsay, E. Y. & Kirsch, D. R. Isolation of the *Candida albicans* gene for orotidine-5'-phosphate decarboxylase by complementation of *S. cerevisiae* ura3 and *E. coli* pyrF mutations. *Mol. Gen.Genet.* **198**, 179-182 (1984).

23 Citiulo, F. *et al. Candida albicans* scavenges host zinc via Pra1 during endothelial invasion. *PLoS Pathogen.* **8**, e1002777 (2012).

24 Gola, S., Martin, R., Walther, A., Dunkler, A. & Wendland, J. New modules for PCR-based gene targeting in *Candida albicans*: rapid and efficient gene targeting using 100 bp of flanking homology region. *Yeast* **20**, 1339-1347 (2003).

25 Wilson, R. B., Davis, D. & Mitchell, A. P. Rapid hypothesis testing with *Candida albicans* through gene disruption with short homology regions. *J. Bacteriol.* **181**, 1868-1874 (1999).

26 Walther, A. & Wendland, J. An improved transformation protocol for the human fungal pathogen *Candida albicans*. *Curr. Genet.* **42**, 339-343, (2003).

27 Murad, A. M., Lee, P. R., Broadbent, I. D., Barelle, C. J. & Brown, A. J. CIp10, an efficient and convenient integrating vector for *Candida albicans*. *Yeast* **16**, 325-327 (2000).

28 Gratacap, R. L., Rawls, J. F. & Wheeler, R. T. Mucosal candidiasis elicits NF-kappaB activation, proinflammatory gene expression and localized neutrophilia in zebrafish. *Dis. Model. Mech.* **6**, 1260-1270 (2013).

29 Moyes, D. L. *et al.* A biphasic innate immune MAPK response discriminates between the yeast and hyphal forms of *Candida albicans* in epithelial cells. *Cell Host Microbe* **8**, 225-235 (2010).

30 Moyes, D. L. *et al. Candida albicans* yeast and hyphae are discriminated by MAPK signaling in vaginal epithelial cells. *PLoS ONE* **6**, e26580 (2011).

31 Wachtler, B., Wilson, D., Haedicke, K., Dalle, F. & Hube, B. From attachment to damage: defined genes of *Candida albicans* mediate adhesion, invasion and damage during interaction with oral epithelial cells. *PloS one* **6**, e17046, (2011).

32 Trinh le, A. *et al.* A versatile gene trap to visualize and interrogate the function of the vertebrate proteome. *Gen. Dev.* **25**, 2306-2320, (2011).

33 Solis, N. V. & Filler, S. G. Mouse model of oropharyngeal candidiasis. *Nat. Protoc.* **7**, 637-642 (2012).

34 Cranfield, C. G. *et al.* Transient potential gradients and impedance measures of tethered bilayer lipid membranes: pore-forming peptide insertion and the effect of electroporation. *Biophys. J.* **106**, 182-189, (2014).

35 Cranfield, C., Carne, S., Martinac, B. & Cornell, B. The assembly and use of tethered bilayer lipid membranes (tBLMs). *Methods in molecular biology (Clifton, N.J.)* **1232**, 45-53, (2015).

36 Schromm, A. B. *et al*. Lipopolysaccharide-binding protein mediates CD14-independent intercalation of lipopolysaccharide into phospholipid membranes. *FEBS Lett* **399**, 267-271 (1996).

37 Chen, G. C. & Yang, Y. T. Two-point calibration of circular dichrometer with D-10-camphorsulfonic acid. *Anal. Lett* **10**, 1195-1207 (1977).

38 Montal, M. & Mueller, P. Formation of bimolecular membranes from lipid monolayers and a study of their electrical properties. *Proc. Natl. Acad. Sci. U S A* **69**, 3561-3566 (1972).

39 Gutsmann, T., Heimburg, T., Keyser, U., Mahendran, K. R. & Winterhalter, M. Protein reconstitution into freestanding planar lipid membranes for electrophysiological characterization. *Nat. Protoc.* **10**, 188-198, (2015).

Extended Data Table references:

40 Gillum, A. M., Tsay, E. Y. & Kirsch, D. R. Isolation of the *Candida albicans* gene for orotidine-5'-phosphate decarboxylase by complementation of *S. cerevisiae* ura3 and *E. coli* pyrF mutations. *Mol. Gen. Genet.* **198**, 179-182 (1984).

41 Wilson, R. B., Davis, D. & Mitchell, A. P. Rapid hypothesis testing with *Candida albicans* through gene disruption with short homology regions. *J. Bacteriol.* **181**, 1868-1874 (1999).

42 Fonzi, W. A. & Irwin, M. Y. Isogenic strain construction and gene mapping *in Candida albicans*. *Genetics* **134**, 717-728 (1993).

43 Davis, D., Wilson, R. B. & Mitchell, A. P. *RIM101*-dependent and-independent pathways govern pH responses in *Candida albicans*. *Mol. Cell. Biol.* **20**, 971-978 (2000).

44 Braun, B. R. & Johnson, A. D. *TUP1*, *CPH1* and *EFG1* make independent contributions to filamentation in *Candida albicans*. *Genetics* **155**, 57-67 (2000).

45 Lo, H. J. *et al.* Nonfilamentous *C. albicans* mutants are avirulent. *Cell* **90**, 939-949 (1997).

46 Moyes, D. L. *et al.* A biphasic innate immune MAPK response discriminates between the yeast and hyphal forms of *Candida albicans* in epithelial cells. *Cell Host Microbe* **8**, 225-235 (2010).

47 Zakikhany, K. *et al. In vivo* transcript profiling of *Candida albicans* identifies a gene essential for interepithelial dissemination. *Cell. Microbiol.* **9**, 2938-2954 (2007).

48 Cao, F. *et al.* The Flo8 transcription factor is essential for hyphal development and virulence in *Candida albicans*. *Mol. Biol. Cell.* **17**, 295-307 (2006).

49 Bockmuhl, D. P., Krishnamurthy, S., Gerads, M., Sonneborn, A. & Ernst, J. F. Distinct and redundant roles of the two protein kinase A isoforms Tpk1p and Tpk2p in morphogenesis and growth *of Candida albicans*. *Mol. Microbiol.* **42**, 1243-1257 (2001).

50 Sonneborn, A. *et al.* Protein kinase A encoded by *TPK2* regulates dimorphism of *Candida albicans. Mol. Microbiol.* **35**, 386-396 (2000).

51 Palmer, G. E., Cashmore, A. & Sturtevant, J. *Candida albicans VPS11* is required for vacuole biogenesis and germ tube formation. *Eukaryot. Cell.* **2**, 411-421 (2003).

52 Zou, H., Fang, H. M., Zhu, Y. & Wang, Y. *Candida albicans* Cyr1, Cap1 and G-actin form a sensor/effector apparatus for activating cAMP synthesis in hyphal growth. *Mol. Microbiol.* **75**, 579-591, (2010).

53 Bates, S. *et al.* Outer chain N-glycans are required for cell wall integrity and virulence of *Candida albicans*. *J. Biol. Chem.* **281**, 90-98 (2006).

54 Murciano, C. *et al. Candida albicans* cell wall glycosylation may be indirectly required for activation of epithelial cell proinflammatory responses. *Infect. Immun.* **79**, 4902-4911 (2011).

55 Murad, A. M. *et al. NRG1* represses yeast-hypha morphogenesis and hypha-specific gene expression in *Candida albicans*. *EMBO J.* **20**, 4742-4752 (2001).

56 Liu, H., Kohler, J. & Fink, G. R. Suppression of hyphal formation in *Candida albicans* by mutation of a *STE12* homolog. *Science* **266**, 1723-1726 (1994).

57 Lane, S., Zhou, S., Pan, T., Dai, Q. & Liu, H. The basic helix-loop-helix transcription factor Cph2 regulates hyphal development in *Candida albicans* partly via *TEC1*. *Mol. Cell. Biol.* **21**, 6418-6428 (2001).

58 White, S. J. *et al.* Self-regulation of *Candida albicans* population size during GI colonization. *PLoS pathogens* **3**, e184 (2007).

59 Brown, D. H., Jr., Giusani, A. D., Chen, X. & Kumamoto, C. A. Filamentous growth of *Candida albicans* in response to physical environmental cues and its regulation by the unique *CZF1* gene. *Mol. Microbiol.* **34**, 651-662 (1999).

60 Kadosh, D. & Johnson, A. D. Rfg1, a protein related to the *Saccharomyces cerevisiae* hypoxic regulator Rox1, controls filamentous growth and virulence in *Candida albicans*. *Mol. Cell. Biol.* **21**, 2496-2505 (2001).

61 San Jose, C., Monge, R. A., Perez-Diaz, R., Pla, J. & Nombela, C. The mitogen-activated protein kinase homolog *HOG1* gene controls glycerol accumulation in the pathogenic fungus *Candida albicans*. *J. Bacteriol.* **178**, 5850-5852 (1996).

62 Firon, A. *et al.* The *SUN41* and *SUN42* genes are essential for cell separation in *Candida albicans*. *Mol. Microbiol.* **66**, 1256-1275 (2007).

63 de Boer, A. D. *et al.* The *Candida albicans* cell wall protein Rhd3/Pga29 is abundant in the yeast form and contributes to virulence. *Yeast* **27**, 611-624 (2010).

64 Muhlschlegel, F. A. & Fonzi, W. A. *PHR2* of *Candida albicans* encodes a functional homolog of the pH-regulated gene *PHR1* with an inverted pattern of pH-dependent expression. *Mol. Cell. Biol.* **17**, 5960-5967 (1997).

65 Martin, R. *et al.* A core filamentation response network in *Candida albicans* is restricted to eight genes. *PloS one* **8**, e58613 (2013).

66 Birse, C. E., Irwin, M. Y., Fonzi, W. A. & Sypherd, P. S. Cloning and characterization of *ECE1*, a gene expressed in association with cell elongation of the dimorphic pathogen *Candida albicans*. *Infect. Immun.* **61**, 3648-3655 (1993).

67 Navarro-Garcia, F., Sanchez, M., Pla, J. & Nombela, C. Functional characterization of the *MKC1* gene of *Candida albicans*, which encodes a mitogen-activated protein kinase homolog related to cell integrity. *Mol. Cell. Biol.* **15**, 2197-2206 (1995).

68 Hausauer, D. L., Gerami-Nejad, M., Kistler-Anderson, C. & Gale, C. A. Hyphal guidance and invasive growth in *Candida albicans* require the Ras-like GTPase Rsr1p and its GTPase-activating protein Bud2p. *Eukaryot. Cell.* **4**, 1273-1286 (2005).

69 Sentandreu, M., Elorza, M. V., Sentandreu, R. & Fonzi, W. A. Cloning and characterization of *PRA1*, a gene encoding a novel pH-regulated antigen of *Candida albicans*. *J. Bacteriol.* **180**, 282-289 (1998).

70 Pardini, G. *et al.* The CRH family coding for cell wall glycosylphosphatidylinositol proteins with a predicted transglycosidase domain affects cell wall organization and virulence of *Candida albicans*. *J. Biol. Chem.* **281**, 40399-40411 (2006).

71 Braun, B. R., Head, W. S., Wang, M. X. & Johnson, A. D. Identification and characterization of *TUP1*-regulated genes in *Candida albicans*. *Genetics* **156**, 31-44 (2000).

72 Fradin, C. *et al.* Granulocytes govern the transcriptional response, morphology and proliferation of *Candida albicans* in human blood. *Mol. Microbiol.* **56**, 397-415 (2005).

73 Staab, J. F., Bradway, S. D., Fidel, P. L. & Sundstrom, P. Adhesive and mammalian transglutaminase substrate properties of *Candida albicans* Hwp1. *Science* **283**, 1535-1538 (1999).

74 Bailey, D. A., Feldmann, P. J., Bovey, M., Gow, N. A. & Brown, A. J. The *Candida albicans HYR1* gene, which is activated in response to hyphal development, belongs to a gene family encoding yeast cell wall proteins. *J. Bacteriol.* **178**, 5353-5360 (1996).

75 Sandini, S., La Valle, R., De Bernardis, F., Macri, C. & Cassone, A. The 65 kDa mannoprotein gene of *Candida albicans* encodes a putative beta-glucanase adhesin required for hyphal morphogenesis and experimental pathogenicity. *Cell. Microbiol.* **9**, 1223-1238 (2007).

76 Csank, C. *et al.* Roles of the *Candida albicans* mitogen-activated protein kinase homolog, Cek1p, in hyphal development and systemic candidiasis. *Infect. Immun.* **66**, 2713-2721 (1998).

77 Hube, B. *et al.* Disruption of each of the secreted aspartyl proteinase genes *SAP1*, *SAP2*, and *SAP3* of *Candida albicans* attenuates virulence. *Infect. Immun.* **65**, 3529-3538 (1997).

78 Taylor, B. N. *et al.* Induction of *SAP7* correlates with virulence in an intravenous infection model of candidiasis but not in a vaginal infection model in mice. *Infect. Immun.* **73**, 7061-7063 (2005).

79 Schild, L. *et al.* Proteolytic cleavage of covalently linked cell wall proteins by *Candida albicans* Sap9 and Sap10. *Eukaryot. Cell.* **10**, 98-109 (2011).

80 Zhao, X. *et al. ALS3* and *ALS8* represent a single locus that encodes a *Candida albicans* adhesin; functional comparisons between Als3p and Als1p. *Microbiology* **150**, 2415-2428 (2004).

81 Murciano, C. *et al.* Evaluation of the role of *Candida albicans* agglutinin-like sequence (Als) proteins in human oral epithelial cell interactions. *PloS ONE* **7**, e33362 (2012).

82 Zhao, X., Oh, S. H., Yeater, K. M. & Hoyer, L. L. Analysis of the *Candida albicans* Als2p and Als4p adhesins suggests the potential for compensatory function within the Als family. *Microbiology* **151**, 1619-1630 (2005).

83 Zhao, X., Oh, S. H. & Hoyer, L. L. Deletion of *ALS5, ALS6* or *ALS7* increases adhesion of *Candida albicans* to human vascular endothelial and buccal epithelial cells. *Med. Mycol.* **45**, 429-434 (2007).

84 Zhao, X., Oh, S. H. & Hoyer, L. L. Unequal contribution of *ALS9* alleles to adhesion between *Candida albicans* and human vascular endothelial cells. *Microbiology* **153**, 2342-2350 (2007).

85 Timpel, C., Strahl-Bolsinger, S., Ziegelbauer, K. & Ernst, J. F. Multiple functions of Pmt1p-mediated protein O-mannosylation in the fungal pathogen *Candida albicans*. *J. Biol. Chem.* **273**, 20837-20846 (1998).

86 Bates, S. *et al. Candida albicans* Pmr1p, a secretory pathway P-type Ca2+/Mn2+-ATPase, is required for glycosylation and virulence. *J. Biol. Chem.* **280**, 23408-23415 (2005).

87 Hobson, R. P. *et al.* Loss of cell wall mannosylphosphate in *Candida albicans* does not influence macrophage recognition. *J. Biol. Chem.* **279**, 39628-39635 (2004).

960 88 Southard, S. B., Specht, C. A., Mishra, C., Chen-Weiner, J. & Robbins, P. W. Molecular
961 analysis of the *Candida albicans* homolog of *Saccharomyces cerevisiae MNN9*,
962 required for glycosylation of cell wall mannoproteins. *J. Bacteriol.* **181**, 7439-7448
963 (1999).
964 89 Munro, C. A. *et al.* Mnt1p and Mnt2p of *Candida albicans* are partially redundant
965 alpha-1,2-mannosyltransferases that participate in O-linked mannosylation and are
966 required for adhesion and virulence. *J. Biol. Chem.* **280**, 1051-1060 (2005).
967 90 Mio, T. *et al.* Role of three chitin synthase genes in the growth of *Candida albicans*. *J.*
968 *Bacteriol.* **178**, 2416-2419 (1996).
969 91 Mille, C. *et al.* Inactivation of *CaMIT1* inhibits *Candida albicans* phospholipomannan
970 beta-mannosylation, reduces virulence, and alters cell wall protein beta-mannosylation.
971 *J. Biol. Chem.* **279**, 47952-47960 (2004).
972 92 Mille, C. *et al.* Identification of a new family of genes involved in beta-1,2-
973 mannosylation of glycans in *Pichia pastoris* and *Candida albicans*. *J. Biol. Chem.* **283**,
974 9724-9736 (2008).
975 93 Mille, C. *et al.* Members 5 and 6 of the *Candida albicans* BMT family encode enzymes
976 acting specifically on beta-mannosylation of the phospholipomannan cell-wall
977 glycosphingolipid. *Glycobiology* **22**, 1332-1342 (2012).
978 94 Mio, T. *et al.* Cloning of the *Candida albicans* homolog of *Saccharomyces cerevisiae*
979 *GSC1/FKS1* and its involvement in beta-1,3-glucan synthesis. *J. Bacteriol.* **179**, 4096-
980 4105 (1997).
981 95 Mio, T. *et al.* Isolation of the *Candida albicans* homologs of *Saccharomyces cerevisiae*
982 *KRE6* and *SKN1*: expression and physiological function. *J. Bacteriol.* **179**, 2363-2372
983 (1997).
984 96 Staab, J. F. & Sundstrom, P. *URA3* as a selectable marker for disruption and virulence
985 assessment of *Candida albicans* genes. *Trends Microbiol.* **11**, 69-73 (2003).
986 97 Murad, A. M., Lee, P. R., Broadbent, I. D., Barelle, C. J. & Brown, A. J. CIp10, an
987 efficient and convenient integrating vector for *Candida albicans*. *Yeast* **16**, 325-327

988 (2000).

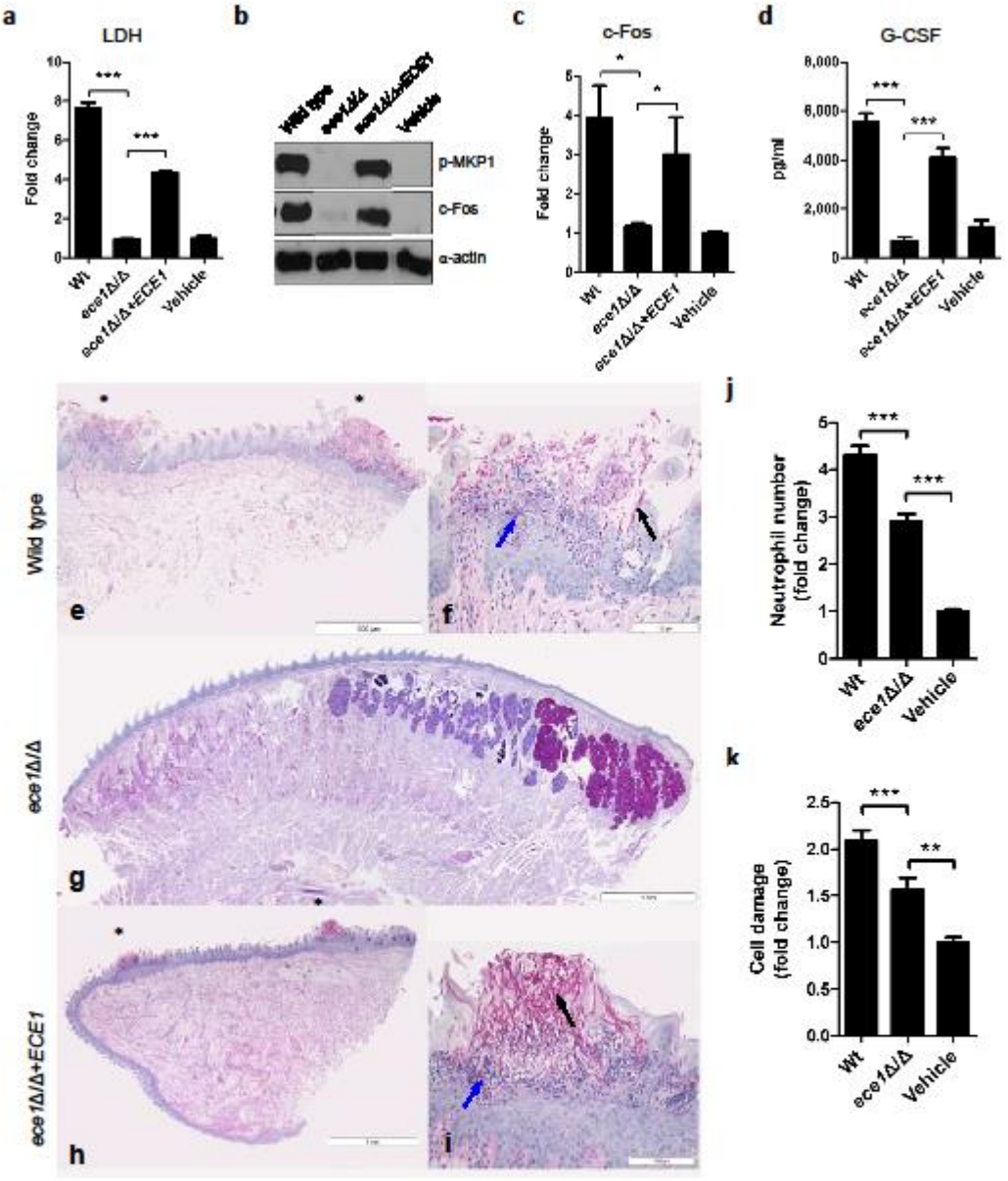

Figure 1

989

990

991

992

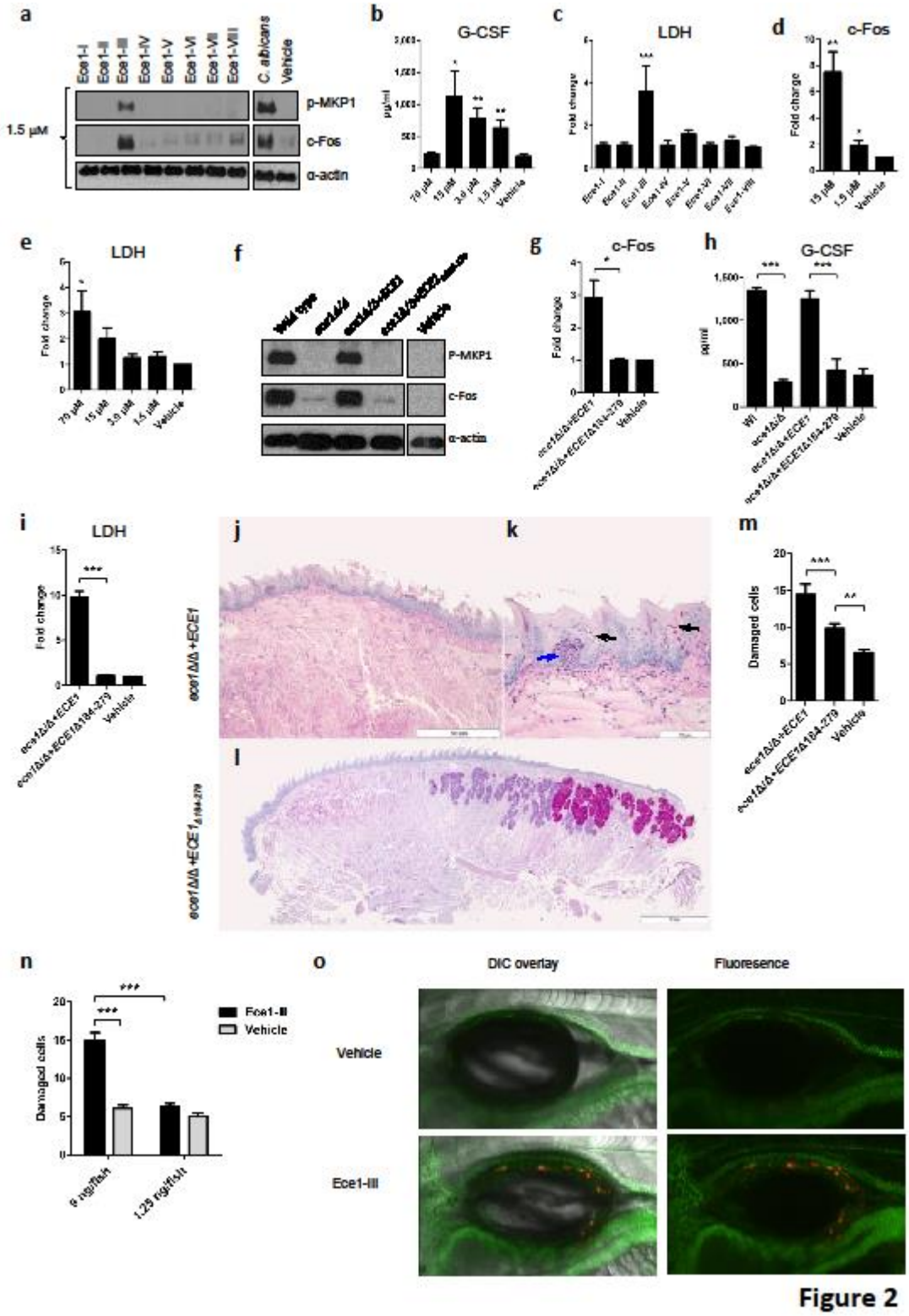
a
Ece1-I
Ece1-II
Ece1-III
Ece1-IV
Ece1-V
Ece1-VI
Ece1-VII
Ece1-VIII
C. albicans
Vehicle
1.5 µM
p-MKP1
c-Fos
α-actin
b
G-CSF
pg/ml
70 µM
15 µM
3.8 µM
1.5 µM
Vehicle
c
LDH
Fold change
d
c-Fos
Fold change
e
LDH
Fold change
f
Wild type
ece1Δ/Δ
ece1Δ/Δ+ECE1
ece1Δ/Δ+ECE1Δ184-279
Vehicle
P-MKP1
c-Fos
α-actin
g
c-Fos
Fold change
ece1Δ/Δ+ECE1
ece1Δ/Δ+ECE1Δ184-279
Vehicle
h
G-CSF
pg/ml
WT
ece1Δ/Δ
ece1Δ/Δ+ECE1
ece1Δ/Δ+ECE1Δ184-279
Vehicle
i
LDH
Fold change
ece1Δ/Δ+ECE1
ece1Δ/Δ+ECE1Δ184-279
Vehicle
j
k
ece1Δ/Δ+ECE1
l
ece1Δ/Δ+ECE1Δ184-279
m
Damaged cells
ece1Δ/Δ+ECE1
ece1Δ/Δ+ECE1Δ184-279
Vehicle
n
Damaged cells
Ece1-III
Vehicle
9 ng/fish
1.25 ng/fish
o
DIC overlay
Fluorescence
Vehicle
Ece1-III

Figure 2

993